# Transcription factor determines the sources of extracellular vesicle DNA

Yunsheng Zhang[1,2], Nana Ding[1], Yizhen Li[1], Xiaoyun Zhao[1], Shiping Yang[1], Ping Fu[1], Yousong Peng[1] Haojie Cheng[1], Min Ouyang[1], Yu Wang[1], Hanyun Liu[1], Yan Chen[1], Xiaoqin Huang[1], Li Yu[1], Yongjun Tan[1*]

[1] State Key Laboratory of Chemo/Biosensing and Chemometrics, College of Biology, Hunan Engineering Research Center for Anticancer Targeted Protein Pharmaceuticals, Hunan University, Changsha, Hunan 410082, PR China.

[2] The Second Affiliated Hospital, University of South China, Hengyang, Hunan 421001, PR China.

**** Correspondence to:*** Dr. Yongjun Tan, E-mail: yjtan@hnu.edu.cn

**Abstract**

Extracellular vesicle DNA (evDNA) acts as a potential mechanism for intercellular communication and possesses an important diagnostic value for multiple diseases. In this study, we have provided the first example that transcription factor determines the sources of evDNA from chromatin DNA. Transcription factor FOXM1 mediates the loading of specific chromatin DNA fragments into extracellular vesicles (EVs). Specifically, certain chromatin DNA fragments are specified by FOXM1 and form LC3-FOXM1-DNA vesicles in cytoplasm during autophagy. Then the cytoplasmic LC3-FOXM1-DNAs are transported to EVs probably through the process of an autophagy-MVB transport. We have confirmed that LC3-FOXM1-DNAs can be absorbed by recipient cells along with the released EVs and certain evDNA fragments integrate into the genome of recipient cells. This discovery provides an understanding for studying the sources and functions of evDNA and helps to expand its application in the future.

**Key words**

Extracellular vesicle DNA; Transcription factor; FOXM1; Autophagy; Extracellular vesicles

Extracellular vesicle DNA (evDNA) carries portions of parent cells' genetic information about the physiological or pathological processes and is considered to act as an intercellular messenger or to maintain cellular homeostasis[1,2]. Although extensive studies have declared its diagnostic value of diseases, the mechanism of DNA loading in extracellular vehicles (EVs) remains elusive and the outcome of evDNA is rarely discussed. Here we show that a transcription factor-involved machinery specifies chromatin DNA certain fragments into EVs and consequently the released evDNA can be absorbed by other cells, providing a plausible mechanism by which a cell releases evDNA to affect other cells. Forkhead Box M1 (FOXM1), a typical proliferation-associated transcription factor[3], can enhance the loading of specific chromatin DNA fragments into EVs through interacting with LC3 during autophagy induced by different conditions. LC3, also called MAP1LC3B or LC3B, is a key member of Atg8 protein family regulating autophagy[4] and has been found to locate in nucleus and associate with chromatin[5]. We show that certain chromatin DNA fragments, FOXM1, and LC3 together can form vesicles in cytoplasm and eventually are released in EVs. The FOXM1-LC3 interaction is required for chromatin DNA becoming evDNA because inhibiting FOXM1-LC3 interaction or autophagy per se diminishes the evDNA loading. Our study suggests that transcription factor FOXM1 can determine the sources of evDNA from chromatin DNA, providing an example of evDNA biogenesis to understand its sources and potential functions.

**The formation of LC3-FOXM1-DNA vesicles in cytoplasm during autophagy**

Autophagy (macroautophagy) is a unique membrane trafficking process that not only regulates the degradation of cellular components [6] but also facilitates the secretion of cellular cargos[7,8]. The autophagic protein LC3 is found to specify the loading of proteins and RNAs into EVs[9]. However, whether nuclear LC3 mediates the secretion of chromatin DNA is not well known. First, we observed

that LC3-FOXM1-DNA vesicles formed in cytoplasm of human lung carcinoma epithelial A549 cells during autophagy induced by different conditions such as starvation, rapamycin, $H_2O_2$, or DNA damage reagent etopside (**Fig. 1a, Extended Data Fig. 1a**). The phenomena were also observed in other human cells such as breast cancer MDA-MB-231 and MCF-7 cells, and human embryonal kidney HEK293T cells (**Extended Data Fig. 1b, c**). The appearance of LC3-FOXM1-DNA vesicles during autophagy correlated with the accumulation of double-stranded DNA in cytoplasm (**Fig. 1b**). After introduced into cells, the exogenous RFP-FOXM1 and GFP-LC3 proteins co-localized in the chromatin DNA-containing cytoplasmic vesicles (**Extended Data Fig. 1d, e**). The RFP-FOXM1 ΔDBD proteins, in which FOXM1-DNA binding domain (DBD)[10] was deleted, could not existed in the chromatin DNA-containing cytoplasmic vesicles (**Extended Data Fig. 1f**), implicating that the FOXM1 DNA-binding abilities were required for the formation of LC3-FOXM1-DNA vesicles in cytoplasm.

Next, we performed chromatin immunoprecipitation sequencing (ChIP-seq) analysis to obtain FOXM1-associated chromatin DNA sequences (named as M1-ADs), LC3-associated chromatin DNA sequences (named as LC3-ADs), and then identify multiple overlaps (named as LC3-M1-ADs, n=100) between M1-ADs and LC3-ADs (**Fig. 1c, d and Extended Data Fig. 2a, Table S1**). We chose three LC3-M1-ADs (LC3-M1-AD1, LC3-M1-AD2, and LC3-M1-AD3) as examples to perform FOXM1 or LC3 ChIP-qPCR and confirmed the association between these DNA regions and FOXM1 or LC3 (**Fig. 1e and Extended Data Fig. 2b, c**). The DNA-pulldown assays further confirmed that LC3-M1-AD1 could bind to FOXM1 and LC3 proteins (**Extended Data Fig. 3a**). Again, the electrophoretic mobility shift assays (EMSA) demonstrated that FOXM1, LC3, and LC3-M1-AD1 could form an LC3-FOXM1-DNA complex (**Extended Data Fig. 3b**). We performed DNA-FISH experiments and found that the LC3-M1-AD1 could translocated to cytoplasm during autophagy (**Fig. 1f**). Cytoplasmic

DNA of A549 cells were extracted for qPCR to show the increased levels of LC3-M1-ADs in cytoplasm during autophagy induced by starvation (**Fig. 1g**). Together, these data suggested that transcription factor FOXM1 could specify the loading of certain chromatin DNA fragments into cytoplasmic LC3-FOXM1-DNA vesicles during autophagy.

**The interaction between FOXM1 and LC3**

To assess the association between FOXM1 and LC3, we investigated their subcellular localization and found that FOXM1 and LC3 could co-localize in nucleus (Pearson Correlation Coefficient value was 0.66 ± 0.08) (**Fig. 2a**). The co-immunoprecipitation (co-IP) experiments revealed that FOXM1 interacted with the lipidated LC3-II[11] in cells (**Fig. 2b and Extended Data Fig. 4a**). A bimolecular fluorescence complementation (BiFC) assay[12] confirmed that the FOXM1-LC3 interaction happened mainly in nucleus (**Fig. 2c**) and relied on the LC3 lipidation, evidenced by that the G120A-mutated LC3 (the lipidation-deficient mutant[5]) lost the abilities of interacting with FOXM1 (**Extended Data Fig. 4b**). The FOXM1-LC3 interaction was further confirmed by the co-IP with exogenous Flag-FOXM1 and GFP-LC3 proteins (**Extended Data Fig. 5a**) or by glutathione *S*-transferase (GST)-pulldown assays with recombinant GST-LC3 proteins (**Extended Data Fig. 5b**). The results of co-IP with the exogenous Flag-FOXM1 and the G120A-mutated GFP-LC3 showed again that the deficiency of LC3 lipidation impaired the FOXM1-LC3 interaction (**Extended Data Fig. 6**).

Next, we mapped critical regions mediating the FOXM1-LC3 interaction on FOXM1 and LC3 proteins and first found that the DNA-binding domain of FOXM1 (FOXM1-DBD) was required for LC3 binding to FOXM1 (**Fig. 2d and Extended Data Fig. 7a**) and FOXM1-DBD alone could interact with LC3 in GST-LC3-pulldown assays (**Fig. 2e**). The overexpression of GFP-FOXM1-DBD abolished the endogenous FOXM1-LC3 interaction and impaired autophagy-induced FOXM1-DNA vesiculation

in cytoplasm (**Extended Data Fig. 7b and c**). It is known that so-called LC3-interacting region (LIR) motif existing in LC3' substrate proteins is crucial for selective autophagy[13,14]. We analyzed the protein sequence of FOXM1-DBD and identified four LIR motifs (263-266, 273-276, 307-310 and 317-320), which were evolutionarily conserved among FOXM1s of human, mouse, rat, and macaque (**Extended Data Fig. 8a**). We generated four FOXM1-DBD mutants (Y263A, F273A, F307A and Y317A, corresponding to the four LIR motifs respectively) and determined that the LIR motif (317-320) in FOXM1-DBD was necessary for LC3 binding to FOXM1 (**Fig. 2f**). Rosetta Flex ddG[15] alanine-scanning analysis was performed with the amino acid sequence of the LIR motif (317-320) and LC3 protein structure[16], and predicted that the Y317A mutation significantly elevated the free energy of binding and consequently disrupted the interaction between this LIR motif and LC3 (**Extended Data Fig. 8b**). The residues R10 and R11, F52, or G120 of LC3 have be identified to contribute for the interaction of LC3 with other proteins[5,17] (**Extended Data Fig. 9a**). Besides the residue G120 of LC3 discussed above, the aa29-128 region (containing F52) of LC3 was required for the FOXM1-LC3 interaction but the aa1-28 region (containing R10 and R11) of LC3 was not (**Extended Data Fig. 9b**). Thus, we generated an LC3 F52A mutant and found that this mutant could not interact with FOXM1, similar as the LC3 G120A mutant (**Extended Data Fig. 9c**). Rosetta Dock[18] was performed with the known structures of FOXM1-DBD[19] and LC3 to simulate the FOXM1-LC3 interaction and predict the formation of potential hydrogen bonds between the LIR motif (317-320) of FOXM1 and the residue F52 of LC3 (**Extended Data Fig. 9d**).

**The cytoplasmic translocation of FOXM1 during autophagy**

To understand the fate of LC3-FOXM1-DNA vesicles, we tracked and confirmed the cytoplasmic translocation of FOXM1 during autophagy (**Fig. 3a, b and Extended Data Fig. 10, 11a**). After

introduced into cells, the exogenous RFP-FOXM1 also translocated to cytoplasm during autophagy (**Fig. 3c and Extended Data Fig. 11b, c**). The FOXM1-LC3 interaction relied on LC3 lipidation (see above) and the lipidated LC3-II could be an autophagosomal marker, being present as dots in cytoplasm in confocal imaging[11] (**Extended Data Fig. 12a, b**). As expected, we found that the co-localized dots of FOXM1 and LC3 in cytoplasm were dramatically increased during starvation-induced autophagy (**Fig. 3d and Extended Data Fig. 12c**). These data suggested that FOXM1 could translocate into cytoplasmic autophagosomes through a lipidated LC3-II-mediated mechanism during autophagy.

Although autophagosomes mediate the degradation of cellular components by fusing with lysosomes[20,21], accumulating evidences prove that they can fuse with multivesicular bodies (MVBs) for the secretion of cellular cargos[9,22,23]. Moreover, MVBs contain subpopulations of LC3-positive intraluminal vesicles (ILVs) during autophagy[9]. It's well known that MVBs generally fuse with plasma membrane to release ILVs that are then called exosomes, a major type of EVs[24]. To test whether FOXM1 existed in MVBs, we immuno-stained the cells with the antibodies of FOXM1 and CD63 (an MVB specific marker[25]) and detected elevated levels of the co-localized dots of FOXM1 and CD63 in cytoplasm during autophagy (**Fig. 3e, and Extended Data Fig. 13a**). Furthermore, we also found that the co-localization of FOXM1 and CD47 (an LC3-associated EV marker[26]) existed in cytoplasm during autophagy (**Extended Data Fig. 13b and c**). Together, these results indicated that the cytoplasmic translocation of FOXM1 occurred during autophagy, probably through an autophagy-MVB transport process.

**The presence of LC3-FOXM1-DNAs in EVs**

To confirm that cytoplasmic LC3-FOXM1-DNAs finally existed in EVs, we first tested whether

FOXM1 and LC3 proteins were present in EVs, with the collected EV samples by serial differential ultracentrifugation, from which the Large EVs (lEVs) were collected at 15,000×g and the Small EVs (sEVs) were collected at 120,000×g, respectively[27] (**Extended Data Fig. 14a**). sEVs, released by MVBs fusing with plasma membrane, were attracted much more attention than lEVs in previous studies[28,29]. In this study, we mainly focused on sEVs to carry out follow-up research and just named sEVs as EVs, except as specifically mentioned. The collected EVs were characterized in terms of size range (80-250 nm) and morphology via nanoparticle tracking analysis (NTA) and transmission electron microscopy (TEM), respectively (**Extended Data Fig. 14b, c**), and then validated by immunoblotting with the EV markers (TSG101[30], CD47[31]) (**Extended Data Fig. 14d**). Consistent with previous findings[9,27], the lipidated LC3-II was detected in the collected EVs (**Fig. 4a and Extended Data Fig. 15d**). FOXM1 was also present in EVs and showed a higher abundance in sEVs than in lEVs (**Fig. 4a and Extended Data Fig. 15a**). Direct Immunoaffinity Capture (DIC) approach, designed to purify the specific EVs containing a certain protein[23], was able to purify the FOXM1-specific EVs from A549 cells, the GFP-FOXM1-specific EVs from GFP-FOXM1-expressed HEK293T cells, or the GFP-LC3-specific EVs from GFP-LC3-expressed HEK293T cells (**Extended Data Fig. 15b, c, d**), further proving that both FOXM1 and LC3 were present in EVs.

Next, we extracted the evDNA from the collected EVs and performed the sequencing analysis to obtain EV-associated DNA sequences (named as EV-ADs), and then identify the overlaps (named as LC3-M1-EV-ADs, n=18) between EV-ADs and LC3-M1-ADs (see above) (**Fig. 4b, c and Extended Data Fig. 16a, and Table S2**). We chose five LC3-M1-EV-ADs (LC3-M1-EV-AD1, LC3-M1-EV-AD2, LC3-M1-EV-AD3, LC3-M1-EV-AD4, and LC3-M1-EV-AD5) as examples for following experiments. The results of qPCR assays showed that LC3-M1-EV-ADs were enriched in evDNA during autophagy

(**Fig. 4d**). evDNA was also purified from the FOXM1-, CD47-, and LC3-specific EVs collected through the DIC approach and showed an enrichment of LC3-M1-EV-ADs in these EVs by qPCR (**Fig. 4e, Extended Data Fig. 16b, c**). Furthermore, evDNA was purified from the EVs of GFP-FOXM1-stable expressing HEK293T cells and showed that the elevation of FOXM1 increased the levels of LC3-M1-EV-ADs in the EVs (**Fig. 4f**). As expected, the knockdown or knockout of FOXM1 had the opposite effects to the levels of LC3-M1-EV-ADs in the EVs (**Fig. 4g and Extended Data Fig. 17a**). Finally, the direct images of EVs were captured to confirm the co-localization of DAPI-stained evDNA signals and RFP-FOXM1 fluorescent signals in the DIC-collected FOXM1-specific EVs (**Extended Data Fig. 17b**).

We further analyzed the effects of the FOXM1-LC3 interaction, which was relied on the LIR motif (317-320) in FOXM1 and F52 residues in LC3 as discussed above, on the loading of LC3-FOXM1-EV-DNAs to EVs. Compared to wild-type FOXM1, the LIR motif Y317A-mutated FOXM1 decreased the levels of LC3-M1-EV-ADs in EVs (**Fig. 4h**). Similarly, LC3 F52A mutant impaired the loading of LC3-M1-EV-ADs to EVs (**Fig. 4i**) and the silencing of LC3 directly inhibited the loading of LC3-M1-EV-ADs to EVs (**Extended Data Fig. 17c**). These data indicated that the FOXM1-LC3 interaction was required for the determination of certain evDNA components and the loading of certain chromatin DNA fragments to EVs. To validate the necessity of autophagy flux on the evDNA loading, we knocked down the levels of Atg7, a key protein for autophagy flux[32], and observed the down-regulated levels of LC3-M1-EV-ADs in EVs (**Extended Data Fig. 17d**). It's known that inhibiting the autolysosomal process in cells could enhance the fusion between autophagosomes and MVBs to secret cellular cargos[33]. Therefore, we tested the effects of chloroquine (CQ), an autolysosome inhibitor[34], on the loading of evDNA and observed the elevation of LC3-M1-EV-ADs in

the EVs of CQ-treated cells during autophagy (**Extended Data Fig. 17e**). Together, these data suggested that the cytoplasmic LC3-FOXM1-DNAs were loaded to EVs during autophagy through an autophagy-MVB transport process.

**The absorption of EVs' LC3-M1-EV-ADs by other cells**

To explore the outcome of evDNA, we first tested whether the EVs of parent cells could be absorbed by other cells. First, the collected EVs were labeled with the red fluorescent DiI dye (a membrane-lipophilic chemical[35]) and incubated with A549 cells. The DiI dye alone could only stain the cellular membrane without entering cells (**Extended Data Fig. 18**) while the red fluorescent dots were detected in cytoplasm of the cells treated with the DiI-labeled EVs (**Fig. 5a**), demonstrating the absorption of EVs by the cells. Then, the DIC-collected GFP-FOXM1-specific EVs were incubated with A549 cells, and the cell samples were immune-stained with anti-GFP antibody and imaged to show the absorption of the EVs' GFP-FOXM1 proteins by the cells (**Fig. 5b**). Interestingly, we detected the DAPI-stained DNA signals, which were co-localized with GFP-FOXM1 proteins, in the cells treated with the GFP-FOXM1-specific EVs, implicating that LC3-M1-EV-ADs might be also absorbed by the cells (**Fig. 5c**). To make sure the absorption of the LC3-M1-EV-ADs by other cells, we selected insect *Spodoptera frugiperda* SF-9 cells as the recipient cells of human EVs because it's easy to distinguish human DNA from insect genome sequences. SF-9 cells were incubated with the EVs of human A549 cells and the DNA samples of SF-9 cells were prepared one or three days later. PCR analyses confirmed that LC3-M1-EV-ADs were absorbed by SF-9 cells (**Fig. 5d**). In order to track the end of LC3-M1-EV-ADs in the recipient cells, we cultured the human EVs-treated SF-9 cells for a long period according to the regular cell culture procedure, and then extracted the genomic DNA from the cells at Week 1 or Week 4 post the EV treatment. Surprisingly, human LC3-M1-EV-ADs could be

detected by PCR analyses in the genomic DNA samples of the SF-9 cells even after 4 weeks of the EV treatment (**Fig. 5e**), implicating that these evDNA might integrate into the genome of the recipient cells.

## Discussion

In this study, we have discovered that transcription factor FOXM1 mediates the loading of specific chromatin DNA fragments into EVs during autophagy. Specifically, certain chromatin DNA fragments are specified by FOXM1 and form LC3-FOXM1-DNA vesicles in cytoplasm. Then the cytoplasmic LC3-FOXM1-DNAs are released in EVs probably through the process of an autophagy-MVB transport, providing an example of the transcription factor determining the sources of evDNA from chromatin DNA (**Fig. 5f**). EVs are a heterogeneous group of cell-derived membranous structures containing DNAs, RNAs, proteins, and lipids[23], which are now considered as an additional mechanism for intercellular communication, allowing cells to exchange genetic materials, proteins, and lipids[24]. Although the biological functions of evDNA are not as deeply explored as that of RNAs and proteins in EVs, the diagnostic value of evDNA has been extensively assessed for multiple diseases[1,2]. There is reason to believe that clarifying the sources of evDNA will help improve its more reliable diagnostic applications. FOXM1 can theoretically specify its binding regions in chromatin directly through its DNA-binding consensus sequence[36] or indirectly through interacting with other transcription factors such as B-Myb, MuvB, and NFY[37], providing a clue to determine the sources of evDNA from certain chromatin DNA regions. Based on this understanding, the accuracy and specificity of disease diagnosis can be improved in the future by focusing on specific sequences in evDNA sequencing data. In addition, the further enrichment analysis of the specific sequences of evDNA can predict certain proteins bound to the sequences, so as to help us to establish the association between the proteins and diseases and

deduce the course or progression of the diseases.

The specificity of the sources of evDNA from chromatin DNA also implicates that evDNA plays a role to transmit specific genetic information between cells. In this study, we have found that the certain chromatin DNA fragments of human A549 cells can be detected in the genomic DNA samples of insect *Spodoptera frugiperda* SF-9 cells treated with the A549-derieved EVs after four weeks, providing an example that evDNA mediates the exchange of genetic information among different cells. Imagining that evDNA-containing EVs of certain cells are able to enter the circulatory system and travel far, we have reason to believe that evDNA may possess important biological roles in exchanging genetic information among tissues. This is an attractive hypothesis that needs further study. In addition, the presence of cytoplasmic DNA can drive cell-autonomous responses such as innate immune activation[38], implicating that evDNA may mediate inflammation of recipient cells. Furthermore, certain extrachromosomal chromatin particles containing extrachromosomal DNA (ecDNA) and RNA Polymerase II have been identified recently to act as mobile transcriptional enhancers to amplify the genome-wide gene transcription in cancer cells[39,40]. In this study, we notice that FOXM1 and the FOXM1-bound evDNA co-exist in EVs of donor cells and are released together from the EVs into recipient cells through mechanisms as yet unknown. Thus we speculate that evDNA-FOXM1 particles formed by FOXM1 and the FOXM1-bound evDNA may function as mobile enhancers in recipient cells through the similar mechanisms of extrachromosomal chromatin particles.

Although this study focuses on FOXM1 as an example to show that transcription factors determine the sources of evDNA from certain chromatin DNA regions, we anticipate that the FOXM1-LC3 interaction is not an isolated event in nucleus and many other transcription factors can act similarly. We have found that other Forkhead Box transcription factors such as FOXA2 and FOXP2

can interact with LC3 (**Extended Data Fig. 19**), implicating that these two transcription factors may also participate in determining the sources of evDNA from chromatin DNA during autophagy. In addition, LC3 interacts with multiple transcription factors and EVs contain many transcription factors, both identified by mass spectrometry analysis[9,27], suggesting that these transcription factors may also play a similar role as FOXM1 for specifying evDNA from chromatin DNA. Transcription factors are generally considered to bind to specific DNA regions of chromosome and regulate specific gene expression in nucleus[41]. Based on the fact that FOXM1 interacts with LC3 to determine the sources of evDNA, the findings of this study expand the understanding of the functions of transcription factors and provide a new perspective to explore their roles in regulating the composition of EVs' DNA components.

FOXM1 is involved in regulating cell proliferation[42], DNA damage repair[43], cell stemness[44], and metastasis[45,46] through stimulating gene transcription in nucleus[10]. The further research on the association among FOXM1, evDNA, and EVs may update the understanding of how FOXM1 performs its various functions. More importantly, one key question that still remains to be answered is how chromatin DNA breaks to generate specific fragments. So far, the formation of chromatin DNA in cytoplasm is considered mainly through the micronuclei and cytoplasmic chromatin fragment pathways[38], but both cannot determine the specificity of chromatin DNA breakage. Although LC3 is found to interact with nuclear LaminB1 protein in nucleus and result in the cytoplasmic translocation of transcriptionally inactive heterochromatin DNA during autophagy[5], the mechanism by which specific DNA fragments break off chromosomes has not been explored. Recently, the complex of Rec114, Mei4 and Mer2 in yeast has been reported to execute and control DNA breakage[47], suggesting that the breaking of specific chromatin DNA can be precisely achieved. Future studies of FOXM1's interaction

with the controlled DNA breakage machinery will help reveal how relevant chromatin DNA fragments are produced. On the other hand, although there is no evidence so far, certain chromatin DNA fragments produced by FOXM1-LC3 may act as ecDNA directly in nucleus. Therefore, investigating FOXM1-LC3-mediated specific chromatin DNA breakage in the future will not only help to clarify the sources of evDNA but also provide clues to answer whether certain transcription factors such as FOXM1 are involved in the ecDNA generation.

## Materials and Methods

**The complete Materials and Methods were described in Supplementary Materials.**

**ChIP sequencing, evDNA sequencing, Bioinformatics analysis, RT-qPCR.** For sequencing, ChIP and evDNA samples were prepared as described previously[48]. The ChIP and evDNA were then purified and used for constructing sequencing libraries with a NEBNext Ultra DNA Library Prep Kit for Illumina (New England Biolabs, Ipswich, MA, USA). The library quantifications were assessed on the Agilent Bioanalyzer 2100 system. The library preparations were sequenced on an Illumina Hiseq platform and 50 bp single-end reads or 150 bp paired-end reads were generated.

For bioinformatics analysis, the following pipeline was used for analysis of all sequence data sets. Firstly, fastp (version 0.20.0, parameter: '-q 15 -u 40 -n 6 -l 15 ')[49] was used to trim adaptors and low-quality reads. Then, we evaluated the quality of NGS short reads by searching them on the FastQC (version 0.11.8) program (http://www.bioinformatics.babraham.ac.uk/projects/fastqc). Thirdly, since ChIP-Seq and evDNA-Seq interrupted fragments were usually small and the percentage of unique sequences in the total number of sequences was the focus of attention, the remaining reads were aligned to human genome hg38 by bwa men (version 0.7.17,parameter: '-t 20')[50]. Finally, peak calling of the aligned reads was made using macs3 (version 3.0.0a6, parameter: '-f BAM -g hs -q 0.1 -B')[51]. Browser views of peaks are shown using Integrated Genomics Viewer (IGV; broadinstitute.org/igv)[52].

For RT-qPCR, the following primers were used for qPCR analyses of LC3-M1-ADs. LC3-M1-AD1 (chr12): forward, 5'-CCA CTT TGA TGG GTC TCG CT-3'; reverse, 5'-TGT CTG GTG ACC GTT GGT TC-3'. LC3-M1-AD2 (chr12): forward, 5'-GAT GGT GTG TGG CTG TAA CAT-3'; reverse, 5'-CTG TGG CCG TGT AAG GCT AT-3'. LC3-M1-AD3 (chr10): forward, 5'-GGG ATA TGT GAA AAC GCC CC-3'; reverse, 5'-CTG CCT ACA GGG AAT TTC GA-3'.

The following primers were used for qPCR analyses of LC3-M1-EV-ADs. LC3-M1-EV-AD1 (chr12) is the same as LC3-M1-AD1; LC3-M1-EV-AD2 (chr10) is the same as LC3-M1-AD3; LC3-M1-EV-AD3 (chr8): forward, 5'-GTT TTC ACA GCC ACT GCA GG-3'; reverse, 5'-ACT CCC GTC AGA GCA ACA TG-3'. LC3-M1-EV-AD4 (chr4): forward, 5'-TCA CAA GCC CCC TGT AGG-3'; reverse, 5'-TCC AAC TCT TGC CTG GTC TC-3'. LC3-M1-EV-AD5 (chr5): forward, 5'-TTC ACG TTT CCC TCA CCC AG-3'; reverse, 5'-TGA GAC ATT TTA CGA AGT TGA GCA-3'.

**DNA Fluorescence *in situ* hybridization (FISH).** DNA-FISH probes were constructed by Exon Biotechnology Inc (Guangzhou, China). The probes covered genomic regions (hg19) used in this study is as follow: chr12: 2853923-2864350 (hg19_ LC3-M1-AD1_10 Kb).

For fluorescence *in situ* hybridization assay, DNA FISH was performed as described[53]. Briefly, coverslips containing fixed and permeabilized cells were quenched by 3% $H_2O_2$, followed by dehydration in 70%, 85%, and 100% ethanol for 1 min each. FISH probe (hg19_ LC3-M1-AD1_10 Kb) was added onto a glass slide, and lower the coverslips onto the slide slowly. Place the slides with samples to be hybridized in a heating block at 85℃ for 5min, and then 37℃ for 20 hours. The slide was then removed, and the sample was washed with Wash Buffer (1 X, preheated to 73℃) for 2 min. Added blocking buffer onto the hybridized samples and incubated at 37℃ for 30 min. Added primary antibody onto coverslip and incubated at 37℃ for 30 min. The sample was washed with Wash Buffer (1 X, preheated to 45℃) for 5 min. Added secondary antibody onto coverslip and incubated at 37℃ for 30 min. Wash coverslip in Wash Buffer (1x) three times at 45℃ for 5 min. Re-wash once with PBS. Preparation of TSA solution at TSA: 0.15%H2O2: TSA amplification buffer = 1:5:500-1:10:1000. Add TSA solution to coverslip and incubate 5-15min at RT. Wash coverslip in Wash Buffer (1 X) three times for 30 min. Mount coverslip with Anti-fade Fluorescence Mounting Medium (with DAPI, Abcam,

#ab104139).

**Extracellular vesicle isolation.** Cells seeded in 150 mm culture dishes at approximately 80% confluence were incubated with serum-free DMEM for 3 days. The cell-conditioned medium was collected by sequential ultracentrifugation[9,23]. Briefly, the medium was first subjected to a centrifugation at 400 × g for 10 min to remove cells. Next, the supernatant was centrifuged at 2,000 × g for 20 min to remove debris and apoptotic bodies. Then, the supernatant was centrifuged at 15,000 × g for 40 min to obtain large EVs. The resulting large EVs pellet was resuspended in a large volume of PBS buffer followed by ultracentrifugation at 15,000 × g for 40 min to wash the sample. To remove any remaining any large EVs, the media supernatant from the first 15,000 × g step was passed through a 0.22-μm pore PES filter (Millipore, Bedford, MA, USA). This supernatant (pre-cleared medium) was next subjected to ultracentrifugation at 120,000 × g for 4 h in a SW 28 Ti Swinging-Bucket Rotor (Beckman Coulter, Fullerton, CA) to sediment small EVs. The crude small EVs pellet was resuspended in a large volume of PBS followed by ultracentrifugation at 120,000 × g for 4 h to wash the sample. All following centrifugation steps were performed at 4℃. Notably, for the comparison of EVs in different conditions, the results must be corrected by total cell number or total protein concentration to eliminate differences in cell seeding.

**Acknowledgements**

We thank Dr. Zhuoxian Rong of Central South University for help with construction of FOXM1 knockout HEK293T cell line by CRISPR/Cas9 technology; thank Dr. Feng Yu of Hunan University for sharing SF-9 cell line; thank Dr. Jianhui Jiang of Hunan University for help with confocal microscopy. This work was supported by the National Natural Science Foundation of China (grant number 81773169 to Y.T.), China Changsha Development and Reform Commission "Mass entrepreneurship and innovation program" (2018-68) and "Innovation platform construction program" (2018-216).

**Author contributions**

Y.Z. and Y.T. conceived this project. Y.Z., N.D., Y.L., X.Z., S.Y., H.L. and Y.W. performed all of experiments. Y.Z., H.C., P.F., Y.P., L.Y. and T.Y. analyzed ChIP-seq and evDNA-seq. M.O. performed molecular docking simulation. Y.C, L.Y. and X.H. provided administrative and material supports. Y.T. supervised this study. Y.Z. and Y.T. composed the manuscript. All authors reviewed the manuscript and discussed the work.

**Competing interests**

The authors declare no competing interests.

**Supplementary Material**

Supplementary methods, figures and tables.

## References


1 Sina, A. A. *et al.* Methylation dependent gold adsorption behaviour identifies cancer derived extracellular vesicular DNA. *Nanoscale Horiz* **5**, 1317-1323 (2020).

2 Elzanowska, J., Semira, C. & Costa-Silva, B. DNA in extracellular vesicles: biological and clinical aspects. *Mol Oncol* **15**, 1701-1714 (2020).

3 Wierstra, I. & Alves, J. FOXM1, a typical proliferation-associated transcription factor. *Biol Chem* **388**, 1257-1274 (2007).

4 Lee, Y. K. & Lee, J. A. Role of the mammalian ATG8/LC3 family in autophagy: differential and compensatory roles in the spatiotemporal regulation of autophagy. *BMB Rep* **49**, 424-430 (2016).

5 Dou, Z. *et al.* Autophagy mediates degradation of nuclear lamina. *Nature* **527**, 105-109 (2015).

6 Klionsky, D. J. & Emr, S. D. Autophagy as a regulated pathway of cellular degradation. *Science* **290**, 1717-1721 (2000).

7 New, J. & Thomas, S. M. Autophagy-dependent secretion: mechanism, factors secreted, and disease implications. *Autophagy* **15**, 1682-1693 (2019).

8 Ponpuak, M. *et al.* Secretory autophagy. *Curr Opin Cell Biol* **35**, 106-116 (2015).

9 Leidal, A. M. *et al.* The LC3-conjugation machinery specifies the loading of RNA-binding proteins into extracellular vesicles. *Nat Cell Biol* **22**, 187-199 (2020).

10 Sanders, D. A. *et al.* FOXM1 binds directly to non-consensus sequences in the human genome. *Genome Biol* **16**, 130 (2015).

11 Tanida, I., Ueno, T. & Kominami, E. LC3 conjugation system in mammalian autophagy. *Int J Biochem Cell Biol* **36**, 2503-2518 (2004).

12 Hu, C. D. & Kerppola, T. K. Simultaneous visualization of multiple protein interactions in living cells using multicolor fluorescence complementation analysis. *Nat Biotechnol* **21**, 539-545 (2003).

13 Birgisdottir, A. B., Lamark, T. & Johansen, T. The LIR motif - crucial for selective autophagy. *J Cell Sci* **126**, 3237-3247 (2013).

14 Johansen, T. & Lamark, T. Selective Autophagy: ATG8 Family Proteins, LIR Motifs and Cargo Receptors. *J Mol Biol* **432**, 80-103 (2020).

15 Barlow, K. A. *et al.* Flex ddG: Rosetta Ensemble-Based Estimation of Changes in Protein-Protein Binding Affinity upon Mutation. *J Phys Chem B* **122**, 5389-5399 (2018).

16 Kuang, Y. *et al.* Structural basis for the phosphorylation of FUNDC1 LIR as a molecular switch of mitophagy. *Autophagy* **12**, 2363-2373 (2016).

17 Sentelle, R. D. *et al.* Ceramide targets autophagosomes to mitochondria and induces lethal mitophagy. *Nat Chem Biol* **8**, 831-838 (2012).

18 Chaudhury, S. *et al.* Benchmarking and analysis of protein docking performance in Rosetta v3.2. *PLoS One* **6**, e22477 (2011).

19 Littler, D. R. *et al.* Structure of the FoxM1 DNA-recognition domain bound to a promoter sequence. *Nucleic Acids Res* **38**, 4527-4538 (2010).

20 Eskelinen, E. L. & Saftig, P. Autophagy: a lysosomal degradation pathway with a central role in health and disease. *Biochim Biophys Acta* **1793**, 664-673 (2009).

21 Yu, L. *et al.* Termination of autophagy and reformation of lysosomes regulated by mTOR.

*Nature* **465**, 942-946 (2010).

22 Leidal, A. M. & Debnath, J. Emerging roles for the autophagy machinery in extracellular vesicle biogenesis and secretion. *FASEB Bioadv* **3**, 377-386 (2021).

23 Jeppesen, D. K. *et al.* Reassessment of Exosome Composition. *Cell* **177**, 428-445 e418 (2019).

24 van Niel, G., D'Angelo, G. & Raposo, G. Shedding light on the cell biology of extracellular vesicles. *Nat Rev Mol Cell Biol* **19**, 213-228 (2018).

25 Piper, R. C. & Katzmann, D. J. Biogenesis and function of multivesicular bodies. *Annu Rev Cell Dev Biol* **23**, 519-547 (2007).

26 Wang, H. S., Pei, F., Chen, Z. & Zhang, L. Increased Apoptosis of Inflamed Odontoblasts Is Associated with CD47 Loss. *J Dent Res* **95**, 697-703 (2016).

27 Hoshino, A. *et al.* Extracellular Vesicle and Particle Biomarkers Define Multiple Human Cancers. *Cell* **182**, 1044-1061 e1018 (2020).

28 Moller, A. & Lobb, R. J. The evolving translational potential of small extracellular vesicles in cancer. *Nat Rev Cancer* **20**, 697-709 (2020).

29 Gao, Y. *et al.* Small Extracellular Vesicles: A Novel Avenue for Cancer Management. *Front Oncol* **11**, 638357 (2021).

30 Yoshioka, Y. *et al.* Comparative marker analysis of extracellular vesicles in different human cancer types. *J Extracell Vesicles* **2**, eCollection 2013 (2013).

31 Kaur, S. *et al.* CD63, MHC class 1, and CD47 identify subsets of extracellular vesicles containing distinct populations of noncoding RNAs. *Sci Rep* **8**, 2577 (2018).

32 Komatsu, M. *et al.* Impairment of starvation-induced and constitutive autophagy in Atg7-deficient mice. *J Cell Biol* **169**, 425-434 (2005).

33 Fader, C. M. & Colombo, M. I. Autophagy and multivesicular bodies: two closely related partners. *Cell Death Differ* **16**, 70-78 (2009).

34 Mauthe, M. *et al.* Chloroquine inhibits autophagic flux by decreasing autophagosome-lysosome fusion. *Autophagy* **14**, 1435-1455 (2018).

35 Yektaeian, N. *et al.* Lipophilic tracer Dil and fluorescence labeling of acridine orange used for Leishmania major tracing in the fibroblast cells. *Heliyon* **5**, e03073 (2019).

36 Marceau, A. H. *et al.* An order-to-disorder structural switch activates the FoxM1 transcription factor. *Elife* **8**, e46131 (2019).

37 Liu, C., Barger, C. J. & Karpf, A. R. FOXM1: A Multifunctional Oncoprotein and Emerging Therapeutic Target in Ovarian Cancer. *Cancers (Basel)* **13**2021).

38 Miller, K. N. *et al.* Cytoplasmic DNA: sources, sensing, and role in aging and disease. *Cell* **184**, 5506-5526 (2021).

39 Zhu, Y. *et al.* Oncogenic extrachromosomal DNA functions as mobile enhancers to globally amplify chromosomal transcription. *Cancer Cell* **39**, 694-707 e697 (2021).

40 Hung, K. L. *et al.* ecDNA hubs drive cooperative intermolecular oncogene expression. *Nature* **600**, 731-736 (2021).

41 Todeschini, A. L., Georges, A. & Veitia, R. A. Transcription factors: specific DNA binding and specific gene regulation. *Trends Genet* **30**, 211-219 (2014).

42 Fu, Z. *et al.* Plk1-dependent phosphorylation of FoxM1 regulates a transcriptional programme required for mitotic progression. *Nat Cell Biol* **10**, 1076-1082 (2008).

43 Tan, Y., Raychaudhuri, P. & Costa, R. H. Chk2 mediates stabilization of the FoxM1

transcription factor to stimulate expression of DNA repair genes. *Mol Cell Biol* **27**, 1007-1016 (2007).

44 Song, I. S. *et al.* FOXM1-Induced PRX3 Regulates Stemness and Survival of Colon Cancer Cells via Maintenance of Mitochondrial Function. *Gastroenterology* **149**, 1006-1016 e1009 (2015).

45 Xie, Z. *et al.* Foxm1 transcription factor is required for maintenance of pluripotency of P19 embryonal carcinoma cells. *Nucleic Acids Res* **38**, 8027-8038 (2010).

46 Li, D. *et al.* The critical role of dysregulated FOXM1-PLAUR signaling in human colon cancer progression and metastasis. *Clin Cancer Res* **19**, 62-72 (2013).

47 Claeys Bouuaert, C. *et al.* DNA-driven condensation assembles the meiotic DNA break machinery. *Nature* **592**, 144-149 (2021).

48 Kharchenko, P. V., Tolstorukov, M. Y. & Park, P. J. Design and analysis of ChIP-seq experiments for DNA-binding proteins. *Nat Biotechnol* **26**, 1351-1359 (2008).

49 Chen, S., Zhou, Y., Chen, Y. & Gu, J. fastp: an ultra-fast all-in-one FASTQ preprocessor. *Bioinformatics* **34**, i884-i890 (2018).

50 Li, H. Aligning sequence reads, clone sequences and assembly contigs with BWA-MEM. *arXiv* **1303.3997** (2013).

51 Zhang, Y. *et al*. Model-based analysis of ChIP-Seq (MACS). *Genome Biol* **9**, R137 (2008).

52 Robinson, J. T. *et al.* Integrative genomics viewer. *Nat Biotechnol* **29**, 24-26 (2011).

53 Tsuchiya, K. D. Fluorescence in situ hybridization. *Clin Lab Med* **31**, 525-542, vii-viii (2011).

## Figures

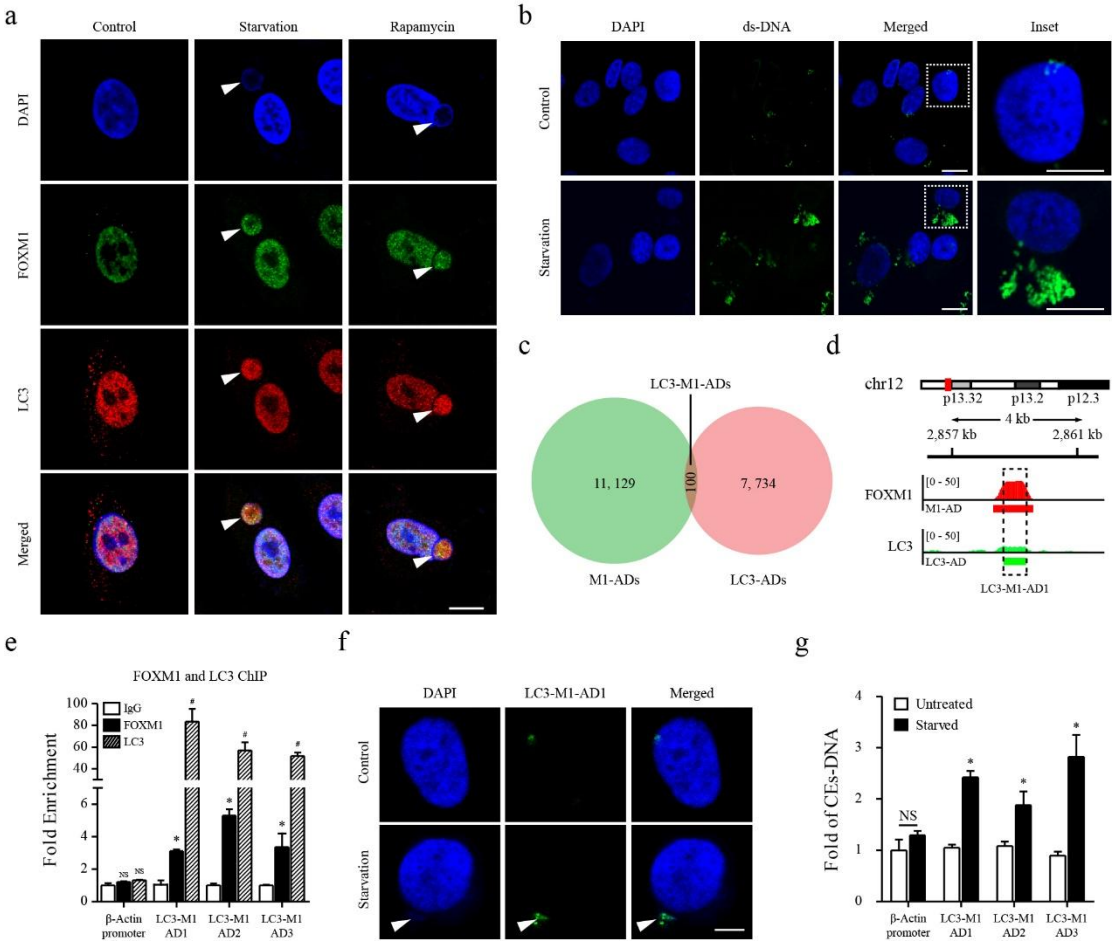


**Figure 1. The formation of LC3-FOXM1-DNA vesicles in cytoplasm during autophagy. (a)** The LC3-FOXM1-DNA vesiculation during autophagy of A549 cells. The white arrows indicate LC3-FOXM1-DNA vesicle. Scale bar, 10 μm. **(b)** The immunofluorescent staining of an anti-dsDNA antibody showed cytoplasmic dsDNA under starvation (6 hrs). Scale bar, 10 μm. **(c)** The overlaps (LC3-M1-ADs, n=100) between M1-ADs (n=11229) and LC3-ADs (n=7834) were identified in genome. **(d)** A representative overlap (LC3-M1-AD1) on chr12 between M1-ADs and LC3-ADs. **(e)** The FOXM1 and LC3 ChIP-qPCR of LC3-M1-ADs in A549 cells. The Bars, mean±s.e.m.; n=3; *$P$<0.05, #$P$<0.05; NS, non-significant; unpaired two-tailed. **(f)** Representative DNA-FISH images of LC3-M1-AD1-adjacent region (10 Kb probe) in A549 cells. The white arrows indicate LC3-M1-AD1. Scale bars, 5 μm. **(g)** A549 cells were treated as indicated and cytoplasmic DNA (CEs-DNA) was

extracted 6 hours later for qPCR. The Bars, mean±s.e.m.; n=3; * $P$<0.05; NS, non-significant; unpaired two-tailed.

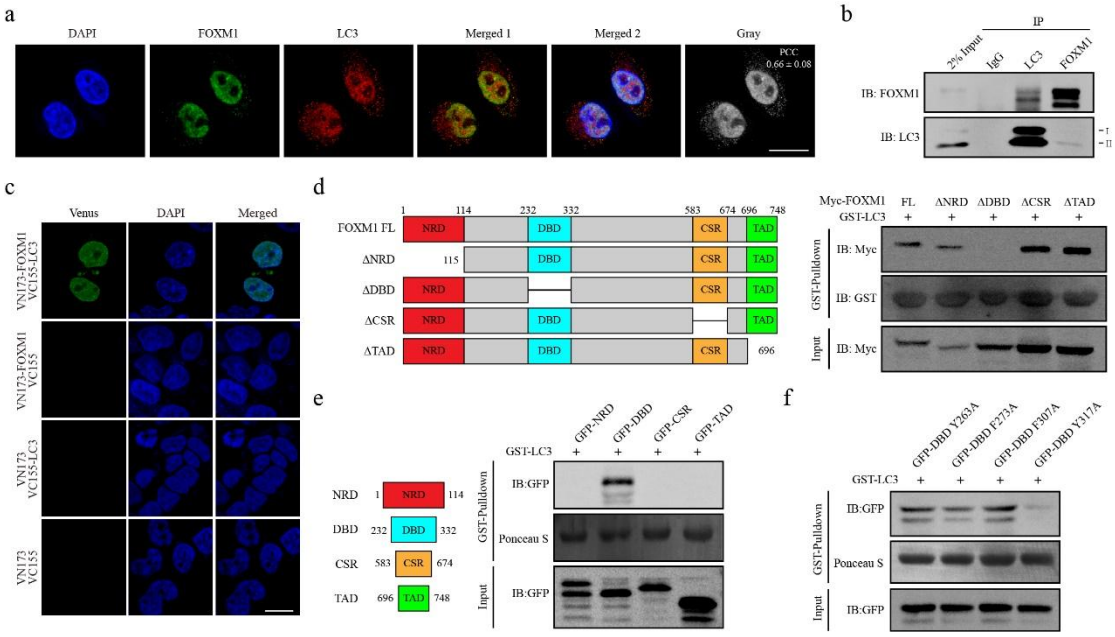


**Figure 2. The interaction between FOXM1 and LC3. (a)** Immunofluorescence staining of FOXM1 and LC3 in A549 cells. Scale bar, 10 μm. The Pearson Correlation Coefficient (PCC) value of FOXM1 and LC3 colocalization was 0.66±0.08. **(b)** Co-immunoprecipitation of endogenous FOXM1 and LC3 in A549 cells. **(c)** The BiFC assays of FOXM1-LC3 interaction. HEK293T cells were transfected with the indicated combination of split Venus constructs for 24 hrs. Scale bar, 10 μm. **(d)** The Myc-tagged FOXM1 deletion mutants were pulled down with bacterially purified GST-LC3 as indicated. **(e)** The GFP-fused FOXM1 truncations were pulled down with bacterially purified GST-LC3 as indicated. **(f)** The GFP-fused FOXM1-DBD point mutations were pulled down with bacterially purified GST-LC3 as indicated.

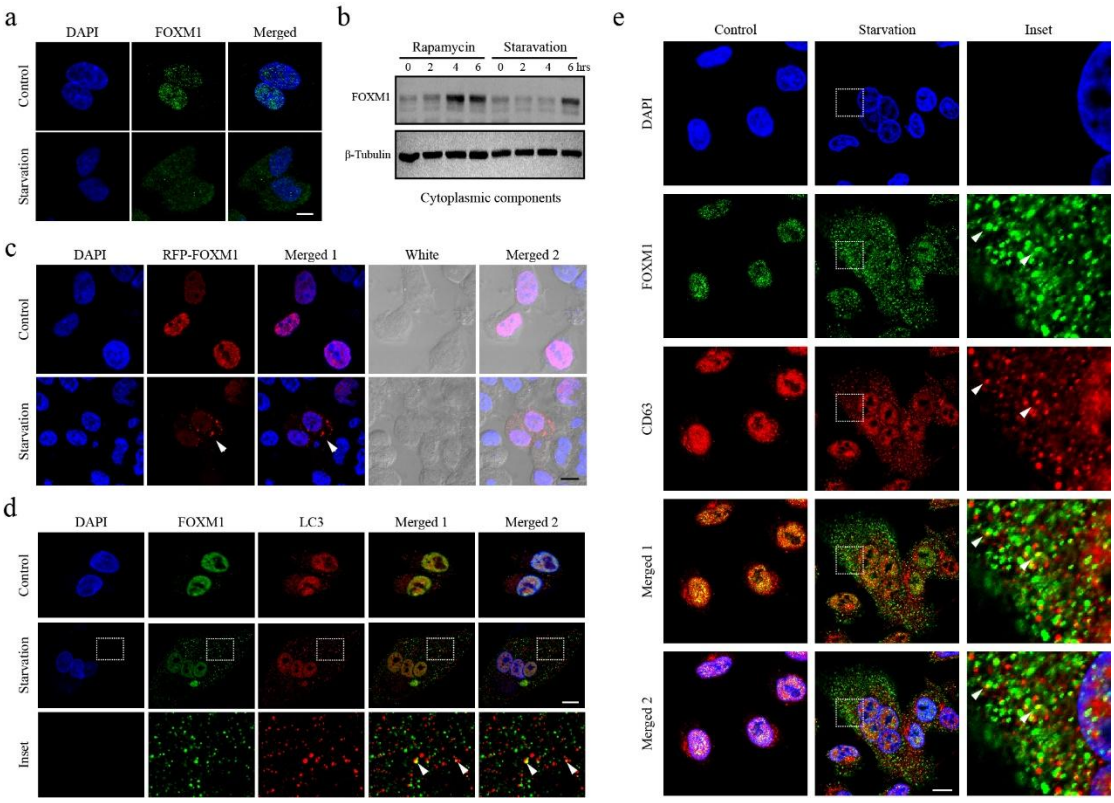


**Figure 3. The cytoplasmic translocation of FOXM1 during autophagy. (a)** Immunofluorescence staining of FOXM1 in A549 cells under starvation (6 hrs). Scale bar, 10 μm. **(b)** A549 cells were treated as indicated and subjected to subcellular fractionation and immunoblotting. **(c)** Exogenous RFP-FOXM1 in HEK293T cells under starvation (6 hrs) was imaged. The white arrows indicate the localization of FOXM1 in cytoplasm. Scale bar, 10 μm. **(d)** Immunostaining of the endogenous FOXM1 and LC3 in A549 cells under starvation (6 hrs). The white arrows indicate the co-localization of FOXM1 and LC3 in cytoplasm. Scale bar, 10 μm. **(e)** Immunostaining of the endogenous FOXM1 and CD63 in A549 cells under starvation (6 hrs). The white arrows indicate the co-localization of FOXM1 and CD63 in cytoplasm. Scale bar, 10 μm.

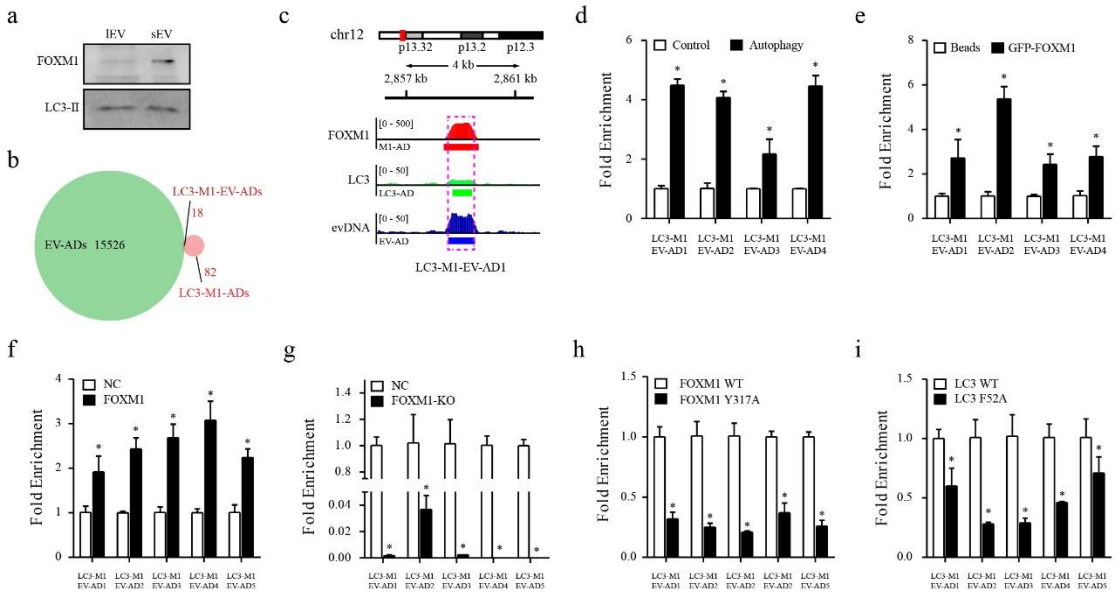


**Figure 4. The presence of LC3-FOXM1-DNAs in EVs. (a)** A549-derived extracellular vesicles were subjected to immunoblotting. lEV, Large extracellular vesicles; sEV, Small extracellular vesicles. **(b)** The overlaps (LC3-M1-EV-ADs, n=18) between EV-ADs (n=15544) and LC3-M1-ADs (n=100) were identified. **(c)** A representative overlap (LC3-M1-EV-AD1) on chr12 between EV-ADs and LC3-M1-ADs. **(d)** The qPCR analyses of LC3-M1-EV-ADs in the EVs collected from A549 cells treated as indicated for 3 days. **(e)** The qPCR analyses of LC3-M1-EV-ADs in the DIC-purified GFP-FOXM1-specific EVs collected from A549 cells. **(f)** The qPCR analyses of LC3-M1-EV-ADs in the EVs collected from FOXM1-overexpressing HEK293T cells. **(g)** The qPCR analyses of LC3-M1-EV-ADs in the EVs collected from FOXM1-knockout HEK293T cells by CRISPR-cas9. **(h)** The qPCR analyses of LC3-M1-EV-ADs in the EVs collected from HEK293T cells that were transfected with FOXM1 WT or Y317A constructs for 3 days. **(i)** The qPCR analyses of LC3-M1-EV-ADs in the EVs collected from HEK293T cells that were transfected with LC3 WT or F52A constructs for 3 days. The Bars, mean±s.e.m.; n=3; *$P < 0.05$; unpaired two-tailed.

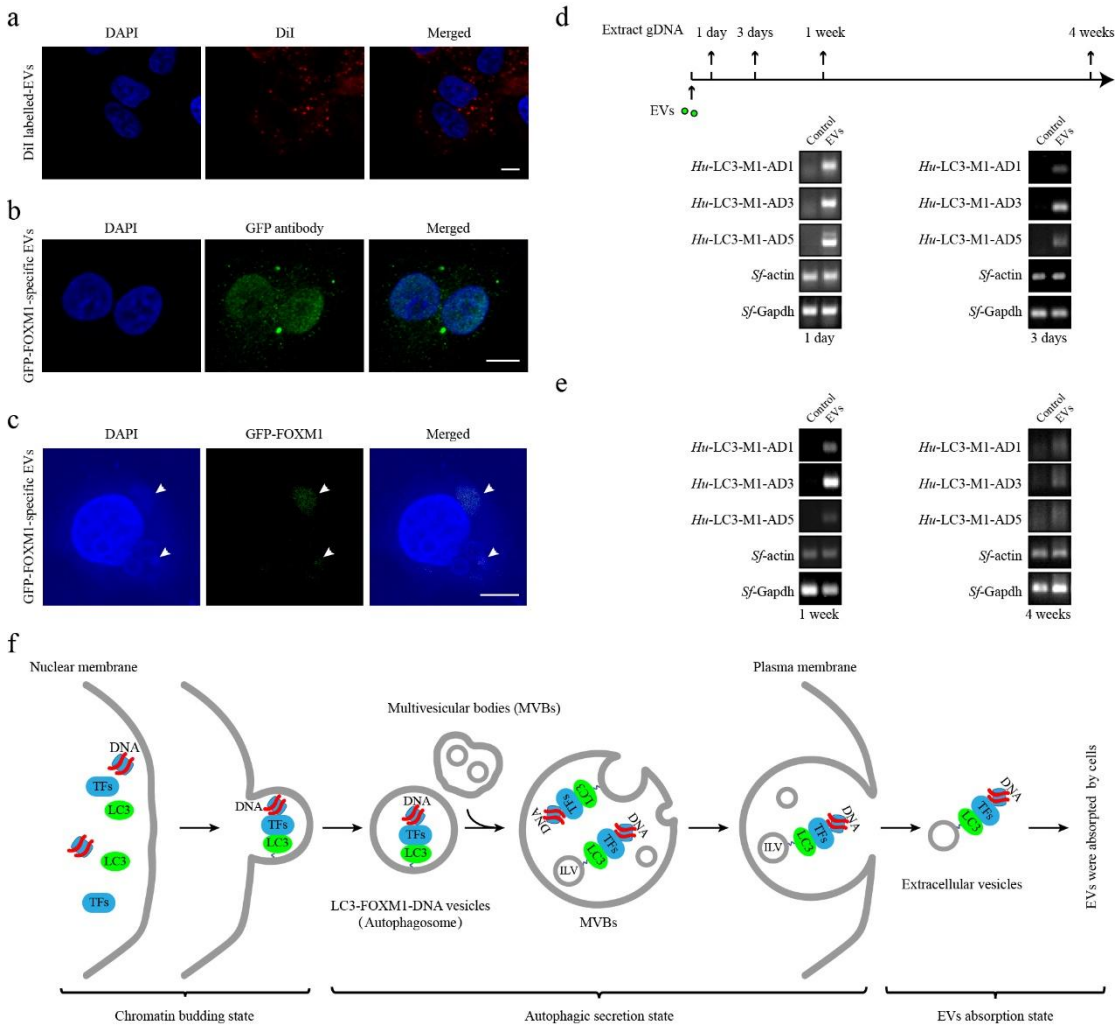


**Figure 5. The absorption of EVs' LC3-M1-EV-ADs by other cells. (a)** Fluorescent imaging of A549 cells incubated 12 hrs with DiI dye-labelled EVs. **(b)** A549 cells were incubated 12 hrs with DIC-purified GFP-FOXM1-specific EVs and immunostained by anti-GFP antibody for fluorescent imaging. **(c)** Fluorescent imaging of A549 cells incubated 12 hrs with DIC-purified GFP-FOXM1-specific EVs. The signals of DAPI were overexposed. Scale bar, 10 μm. **(d)** Insect *Spodoptera frugiperda* SF-9 cells were treated with human A549 cells-derived EVs and one or three days later the genomic DNA was extracted for PCR analyses of human LC3-M1-EV-ADs. **(e)** SF-9 cells were treated as (d) and one or four weeks later the genomic DNA was extracted for PCR analyses of human LC3-M1-EV-ADs. **(f)** Schematic illustration of evDNA biogenesis. TFs, transcription factors.